

Cite this: *Chem. Sci.*, 2021, 12, 1924

All publication charges for this article have been paid for by the Royal Society of Chemistry

Received 13th November 2020

Accepted 11th December 2020

DOI: 10.1039/d0sc06258h

rsc.li/chemical-science

## Intermediates involved in serotonin oxidation catalyzed by Cu bound A $\beta$ peptides†

Arnab Kumar Nath, Arnab Ghatak, Abhishek Dey<sup>ID</sup>\* and Somdatta Ghosh Dey<sup>ID</sup>\*

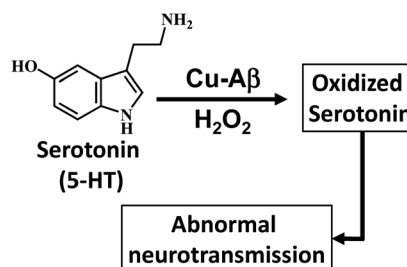
The degradation of neurotransmitters is a hallmark feature of Alzheimer's disease (AD). Copper bound A $\beta$  peptides, invoked to be involved in the pathology of AD, are found to catalyze the oxidation of serotonin (5-HT) by H<sub>2</sub>O<sub>2</sub>. A combination of EPR and resonance Raman spectroscopy reveals the formation of a Cu(II)–OOH species and a dimeric, EPR silent, Cu<sub>2</sub>O<sub>2</sub> bis- $\mu$ -oxo species under the reaction conditions. The Cu(II)–OOH species, which can be selectively formed in the presence of excess H<sub>2</sub>O<sub>2</sub>, is the reactive intermediate responsible for 5-HT oxidation. H<sub>2</sub>O<sub>2</sub> produced by the reaction of O<sub>2</sub> with reduced Cu(I)–A $\beta$  species can also oxidize 5-HT. Both these pathways are physiologically relevant and may be involved in the observed decay of neurotransmitters as observed in AD patients.

## Introduction

Alzheimer's disease (AD) is a terminal neurodegenerative disease which is characterized by the deposition of insoluble plaques in the hippocampus of an AD affected brain.<sup>1,2</sup> It is clinically characterized by progressive dementia.<sup>3</sup> The exact cause for this disease is still unclear. Over the past two decades extensive research has focused on determining the actual cause of this disease, resulting in important hypotheses relating to the pathology of AD. Among them, one of the more accepted hypothesis is the “amyloid hypothesis”.<sup>4–6</sup> The amyloid  $\beta$ -peptide is the main constituent of this hypothesis and is found in high proportions in the plaques that are diagnostic of AD.<sup>5,6</sup> Moreover transition metals like Cu(II) and Zn(II) and cofactors like heme are found in the plaques of an AD brain.<sup>7–9</sup> Apart from the ability of these bivalent metals to aggregate the monomeric A $\beta$  peptides, redox active metals like Cu and Fe are proposed to cause oxidative stress resulting in damage to the neuronal cell membrane making it “leaky”.<sup>7,9</sup> The oxidative damage is proposed to be an upstream event which eventually leads to the formation of insoluble plaques which is a hallmark of the disease.<sup>7,10</sup> The oxidative stress can be due to hydrogen peroxide (H<sub>2</sub>O<sub>2</sub>), which, apart from its natural availability, can also be produced by the reaction of the reduced redox active metals bound A $\beta$  peptides with O<sub>2</sub>.<sup>9,11,12</sup>

The recent investigation of Cu bound A $\beta$  peptides and their site-directed mutants using a combination of spectroscopic techniques and theoretical calculations has revealed a Cu active site coordinated to histidine residues and exchangeable

ligands.<sup>13–18</sup> The Cu–A $\beta$  complexes exhibit peroxidase activity in the presence of H<sub>2</sub>O<sub>2</sub>.<sup>12</sup> Presently several naturally occurring copper containing metalloenzymes are known which can oxidize/hydroxylate organic compounds in the presence of H<sub>2</sub>O<sub>2</sub>. Enzymes like amine oxidase participate in the breakdown of amines to produce an aldehyde and ammonia.<sup>19–21</sup> Alternatively, copper enzymes like dopamine  $\beta$ -hydroxylase (DBH) are involved in the synthesis of a small-molecule neurotransmitter by catalyzing the hydroxylation of dopamine to convert it to norepinephrine.<sup>19,22–24</sup> Note that the Cu active sites of these above-mentioned proteins also have histidine and water derived exchangeable ligands in their active sites similar to that of Cu–A $\beta$ . Now oxidative degradation of neurotransmitters like serotonin generating neurotoxins like tryptamine-4,5-dione is a hallmark of AD, which can lead to impaired neuronal signaling.<sup>25–33</sup> This raises the possibility of Cu bound A $\beta$  reacting with H<sub>2</sub>O<sub>2</sub> and catalyzing the degradation of neurotransmitters (Scheme 1). Previously Ming *et al.* have kinetically shown the catalytic hydroxylation/oxidation of substrates like dopamine, catechol derivatives, phenol and serotonin and proposed a side-on  $\mu$ -peroxo dicopper(II) intermediate as the



Scheme 1 Oxidation of the neurotransmitter serotonin (5-HT) by Cu–A $\beta$  and H<sub>2</sub>O<sub>2</sub>.

Indian Association for the Cultivation of Science, 2A & 2B, Raja S. C. Mullick Road, Jadavpur, Kolkata 700032, India. E-mail: icsgd@iacs.res.in

† Electronic supplementary information (ESI) available. See DOI: 10.1039/d0sc06258h



active species, though no spectroscopic proof was provided.<sup>34–37</sup> Since the oxidation of neurotransmitters by Cu-A $\beta$  in the presence of H<sub>2</sub>O<sub>2</sub> is a likely physiological process occurring in the human brain, the identification and characterization of the reactive intermediates involved in this chemical oxidation process are crucial for the understanding of this disease.

In this manuscript, we experimentally determine the reaction intermediates involved in serotonin oxidation as well as in the peroxidase activity pathway of Cu(II) bound A $\beta$  peptides in the presence of H<sub>2</sub>O<sub>2</sub>. Spectroscopic evidence reveals that two intermediates, Cu<sub>2</sub>O<sub>2</sub>-bis- $\mu$ -oxo and Cu(II)-OOH, are formed in the reaction of Cu-A $\beta$  and H<sub>2</sub>O<sub>2</sub>.

## Results and discussion

### Neurotransmitter serotonin (5-HT) oxidation by Cu-A $\beta$ with H<sub>2</sub>O<sub>2</sub>

The reaction of the neurotransmitter serotonin (5-HT) with Cu-A $\beta$  in the presence of H<sub>2</sub>O<sub>2</sub> produces absorption peaks at 289, 323, 355, 392, 488 and 535 nm (Fig. 1A and S1<sup>†</sup>). These peaks are indicative of serotonin oxidation. Note that, as Cu-A $\beta$  (1–16) and Cu-A $\beta$  (1–40) produce similar serotonin oxidized products, all the other experiments have been performed with Cu-A $\beta$  (1–16). The oxidized products of serotonin are further characterized using HPLC as previously reported (Fig. S2 and Scheme S1<sup>†</sup>).<sup>38,39</sup> The products are found to be tryptamine-4,5-dione (T-4,5-D), 5-hydroxy-3-ethylamino-2-oxindole (5-HEO) and 3,3'-bis(2-aminoethyl)-5-hydroxy-[3,7'-bi-1*H*-indole]-2,4',5'(3*H*)-trione, which is the aerially oxidized dimer of T-4,5-D and 5-HEO.

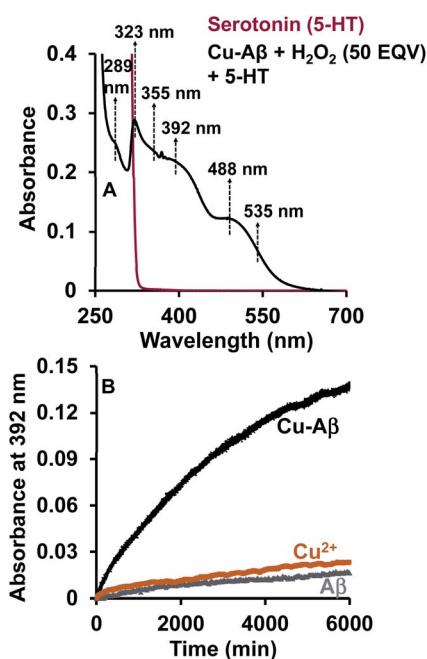
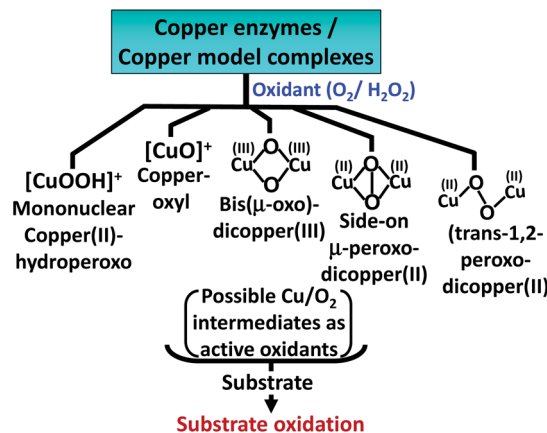


Fig. 1 (A) Absorption spectrum of serotonin (5-HT), red; 5-HT + Cu-A $\beta$  + 50 eq. H<sub>2</sub>O<sub>2</sub>, black; (B) kinetics of serotonin oxidation monitored at 392 nm; 5-HT + Cu-A $\beta$  + 50 eq. H<sub>2</sub>O<sub>2</sub>, black; 5-HT + CuSO<sub>4</sub> + 50 eq. H<sub>2</sub>O<sub>2</sub>, brown; 5-HT + A $\beta$  + 50 eq. H<sub>2</sub>O<sub>2</sub>, grey; in 100 mM HEPES buffer at pH 7. [Cu-A $\beta$  = 0.055 mM, H<sub>2</sub>O<sub>2</sub> = 2.77 mM and 5-HT = 2.77 mM].



Scheme 2 Possible reactive Cu/O<sub>2</sub> intermediates for substrate oxidation by different copper enzymes and copper model complexes in the presence of oxidants (O<sub>2</sub> or H<sub>2</sub>O<sub>2</sub>).<sup>19,40–42</sup>

The pseudo 1<sup>st</sup> order rate for this reaction is found to be  $(4 \pm 0.2) \times 10^{-4} \text{ s}^{-1}$  (Fig. 1B and S3<sup>†</sup>). Note that the slow kinetics of this oxidation matches the slow onset and progression of this disease. Control experiments without Cu-A $\beta$ , *i.e.* H<sub>2</sub>O<sub>2</sub> or Cu(II) (Fenton reaction conditions) alone, show barely any oxidation of 5-HT (Fig. 1B).

The oxidation of 5-HT by H<sub>2</sub>O<sub>2</sub> catalyzed by Cu(II)-A $\beta$  can proceed *via* several reactive intermediates similar to those which have been observed in different Cu enzymatic active sites and their synthetic analogues<sup>19,40–43</sup> (Scheme 2). Hence the reaction of Cu-A $\beta$  with H<sub>2</sub>O<sub>2</sub> is monitored with the aim of trapping and characterizing the active oxidant responsible for oxidizing substrates like serotonin and other neurotransmitters.

### Characterization of Cu/O<sub>2</sub> intermediates formed in the reaction of Cu-A $\beta$ with H<sub>2</sub>O<sub>2</sub>

**Absorption spectroscopy.** At physiological pH, Cu-A $\beta$  shows a broad ligand field band at 630 nm. The addition of H<sub>2</sub>O<sub>2</sub> to Cu-A $\beta$  produces charge transfer (CT) bands at 350 nm ( $\epsilon = 1200 \text{ M}^{-1} \text{ cm}^{-1}$ ) and 411 nm ( $\epsilon = 850 \text{ M}^{-1} \text{ cm}^{-1}$ ) (Fig. 2). The energies of these CT bands are characteristic of peroxide

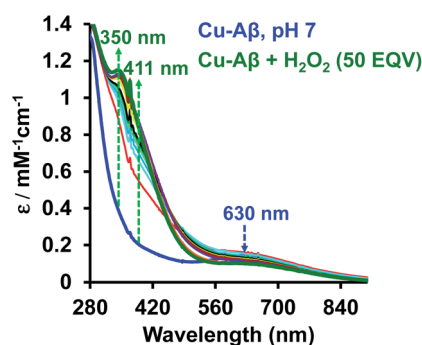


Fig. 2 Absorption spectrum of Cu-A $\beta$ , blue; Cu-A $\beta$  with 50 eq. of H<sub>2</sub>O<sub>2</sub> at different times, green being the final spectrum after 120 minutes; data are collected in 100 mM HEPES buffer at pH 7. The arrows indicate the direction of the spectral changes.



$\pi_v^* \rightarrow \text{Cu LMCT}$ . CT bands in these regions hint at the plausible formation of either a side-on  $\mu$ -peroxo-dicopper(II) complex or a bis( $\mu$ -oxo)dicopper(III) complex as depicted in Scheme 2.<sup>41,42,44–46</sup> Previously Ming and coworkers proposed the formation of a side-on  $\mu$ -peroxo dicopper(II) intermediate.<sup>34,36</sup>

**EPR spectroscopy.** Both side-on peroxo and bis( $\mu$ -oxo) complexes are diamagnetic ( $S = 0$ ) and hence are expected to be EPR silent.<sup>44,47,48</sup> The native Cu-A $\beta$  at pH 7 shows a characteristic ( $S = 1/2$ ) axial EPR signal (predominantly component I with a trace of component II) (Fig. 3A and C).<sup>13,16</sup> When  $\text{H}_2\text{O}_2$  is added to Cu-A $\beta$ ,  $\sim 40\%$  loss of the EPR signal is observed relative to that of the starting Cu-A $\beta$  signal (Fig. 3A and S4 $\dagger$ ). A loss in EPR signal intensity can be indicative of the formation of a diamagnetic side-on  $\mu$ -peroxo-dicopper(II) or a bis( $\mu$ -oxo)dicopper(III) species. The formation of a dimeric species from mononuclear Cu-A $\beta$  should result from the dimerization of two monomeric Cu species. Accordingly, as the Cu-A $\beta$  concentration is doubled, the rate of spin loss of the Cu-A $\beta$  EPR signal is doubled (Fig. 3B). This indicates that the side-on  $\mu$ -peroxo-dicopper(II) or bis( $\mu$ -oxo)dicopper(III) bridging is intermolecular resulting in the formation of a diamagnetic species. Note that in this reaction, the EPR signal of the reaction mixture of Cu-A $\beta$  and  $\text{H}_2\text{O}_2$  did not disappear completely (Fig. 3A). Thus, the remaining spin on Cu-A $\beta$  after the reaction is likely due to the presence of unreacted Cu-A $\beta$  or the formation of another paramagnetic species. The EPR parameters of the residual paramagnetic species ( $S = 1/2$ ,  $g_{\text{II}} = 2.206$ ) (Fig. 3A, C and Table 1) indicate the formation of a distinct species and is not consistent with residual unreacted Cu-A $\beta$ . The new diamagnetic and paramagnetic species observed in absorption and EPR spectroscopy have characteristic vibrations and have been further probed using resonance Raman spectroscopy.

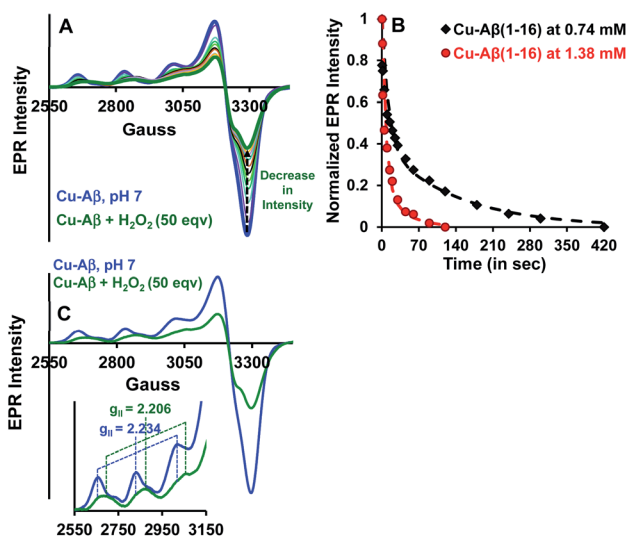


Fig. 3 (A) EPR spectra of Cu-A $\beta$ , blue; Cu-A $\beta$  with 50 eq.  $\text{H}_2\text{O}_2$  at different times, green being the final spectrum after 120 minutes; (B) kinetics of the loss of the EPR signal for 50 eq.  $\text{H}_2\text{O}_2$  with 0.74 mM Cu-A $\beta$ , black and 1.38 mM Cu-A $\beta$ , red; (C) EPR spectra of Cu-A $\beta$ , blue; Cu-A $\beta$  with 50 eq.  $\text{H}_2\text{O}_2$ , green, inset: hyperfine overlay of the data; data are obtained in 100 mM HEPES buffer at pH 7 and 77 K.

Table 1 EPR parameters of Cu-A $\beta$  and a Cu-A $\beta$  + 50 eq.  $\text{H}_2\text{O}_2$  mixture at pH 7

Complex	$A_{\text{II}}$	$g_{\text{II}}$
Cu-A $\beta$	173	2.234
Cu-A $\beta$ + 50 eq. $\text{H}_2\text{O}_2$	166	2.206

**Resonance Raman spectroscopy.** The resonance Raman spectra of the frozen sample of the reaction mixture of Cu-A $\beta$  and  $\text{H}_2\text{O}_2$  is obtained using an excitation wavelength of 415.4 nm at 77 K. The reaction mixture of Cu-A $\beta$  and  $\text{H}_2\text{O}_2$  exhibits resonance Raman bands at 518, 540, 570 and 849  $\text{cm}^{-1}$  (Fig. 4). Bands in the range of 500–600  $\text{cm}^{-1}$  are characteristic of Cu-O vibrations of either a bis( $\mu$ -oxo)copper(III) core or a Cu(II)-OOH species, whereas a band at around 849  $\text{cm}^{-1}$  is characteristic of O-O vibration of a Cu(II)-OOH species.<sup>40–42,49–51</sup> Note that the characteristic Cu-O and O-O vibrations of the side-on  $\mu$ -peroxo-dicopper(II) complex are usually observed at  $\sim 580$  and  $\sim 750$   $\text{cm}^{-1}$  respectively.<sup>41,44</sup> These assignments can be verified by isotopic substitution of the oxygen or proton of  $\text{H}_2\text{O}_2$ . The reaction mixture of Cu-A $\beta$  and  $\text{H}_2\text{O}_2$  in a deuterated medium shows a shift of the bands from 849 and 518  $\text{cm}^{-1}$  to 840 and 512  $\text{cm}^{-1}$  respectively (Fig. 4B). However, the bands at 540 and 570  $\text{cm}^{-1}$  remain unperturbed (Fig. 4A). This H/D shift of the 849 and 518  $\text{cm}^{-1}$  bands is comparable with those

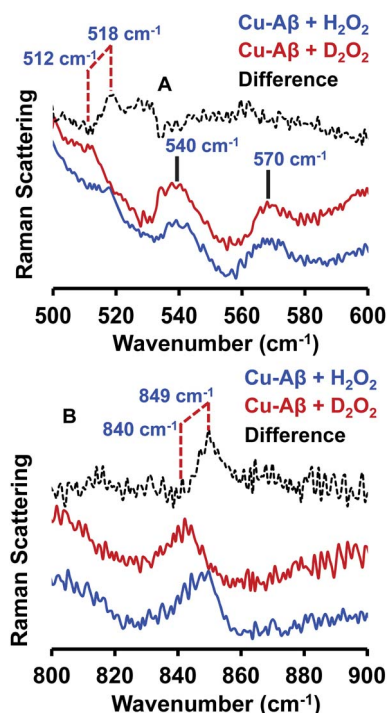
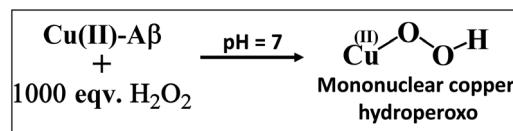


Fig. 4 Resonance Raman spectra of (A) Cu-A $\beta$  + 50 eq.  $\text{H}_2\text{O}_2$ , blue and Cu-A $\beta$  + 50 eq.  $\text{D}_2\text{O}_2$  in, red; difference spectrum of  $\text{H}_2\text{O}_2$  data from  $\text{D}_2\text{O}_2$  data, dashed black; lower energy region; (B) Cu-A $\beta$  + 50 eq.  $\text{H}_2\text{O}_2$ , blue and Cu-A $\beta$  + 50 eq.  $\text{D}_2\text{O}_2$  in, red; difference spectrum of  $\text{H}_2\text{O}_2$  data from  $\text{D}_2\text{O}_2$  data, dashed black; higher energy region. Data were obtained with an excitation wavelength of 415.4 nm (10 mW at the sample) at 77 K (full spectra in Fig. S5 $\dagger$ ).



reported for several Cu–OOH and Fe–OOH species.<sup>51–57</sup> Therefore the 849 cm<sup>−1</sup> band can be assigned to the O–O vibration and the 518 cm<sup>−1</sup> band can be assigned to the Cu–O vibration of a Cu(II)–OOH species of Cu–Aβ, and represents the new paramagnetic species observed in the EPR spectrum (Fig. 3 and Table 1) when H<sub>2</sub>O<sub>2</sub> is added to Cu–Aβ. The two bands at 540 and 570 cm<sup>−1</sup> which do not show any deuterium shift arise from a Fermi resonance (Fig. 4A) and are characteristic Cu–O vibrations of a diamond core bis(μ-oxo) species.<sup>45,48,49</sup> Hence, the doublet in the resonance Raman spectra, CT bands at 350 nm and 411 nm and EPR inactivity (*S* = 0) are all consistent with the formation of a bis(μ-oxo)dicopper(III) species. Thus, Cu–Aβ reacts with H<sub>2</sub>O<sub>2</sub> to generate two different Cu/O<sub>2</sub> species; a bis(μ-oxo)dicopper(III) species and a mononuclear Cu(II)–OOH species as shown in Scheme 3. Note that the *trans*-1,2-peroxo dicopper(II) (Cu–OOCu) could be another possibility but is excluded since the UV-Vis spectrum of Cu–Aβ + H<sub>2</sub>O<sub>2</sub> does not possess any intense band in the range between 480 and 550 nm, which is characteristic of a *trans*-1,2-peroxo dicopper(II) species.<sup>40,41,58,59</sup> Moreover, it has a characteristic O–O vibration in between 800 and 830 cm<sup>−1</sup> which is very low as compared to a mononuclear Cu(II)–OOH species, which shows O–O stretch ranging from 830 to 880 cm<sup>−1</sup>.<sup>40,41,51,52</sup> Most importantly the *trans*-1,2-peroxo species does not show any H/D shift, which is seen in a mononuclear Cu(II)–OOH species.<sup>40,41,51–53,59</sup>

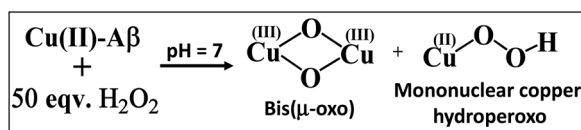
**Active oxidant.** The Cu<sub>2</sub>O<sub>2</sub> bis(μ-oxo)dicopper(III) dimer can be formed by a reaction between two equivalents of Cu–Aβ and one equivalent of H<sub>2</sub>O<sub>2</sub>. Alternatively, Cu–Aβ can react with H<sub>2</sub>O<sub>2</sub> to form Cu(II)–OOH which then dimerizes to Cu<sub>2</sub>O<sub>2</sub> bis(μ-oxo)dicopper(III) in the presence of another Cu–Aβ. We find that when Cu–Aβ reacts with an increased amount of H<sub>2</sub>O<sub>2</sub> (1000 equivalents) keeping everything else the same, the EPR spectrum shows that there is no loss of spin during this reaction (Fig. 5) and parallel rR data do not reveal the formation of the dimeric Cu<sub>2</sub>O<sub>2</sub> bis(μ-oxo)dicopper(III) species. Although the O–O



Scheme 4 Reaction of Cu–Aβ with 1000 eq. H<sub>2</sub>O<sub>2</sub> at pH 7.

vibration of the Cu(II)–OOH species is masked by the O–O vibration of free H<sub>2</sub>O<sub>2</sub> in solution at 890 cm<sup>−1</sup>, the Cu–O vibration and its shift in D<sub>2</sub>O are clearly observed (Fig. S6†). Thus under these reaction conditions, Cu(II)–OOH is formed exclusively (Scheme 4). Interestingly, the oxidation of 5-HT continues to occur under these conditions (Fig. S7, S8 and Table S1†). Note that the use of 1000 eq. H<sub>2</sub>O<sub>2</sub> is not physiologically relevant and the purpose of the experiment is to avoid dimerization and to generate mononuclear Cu(II)–OOH exclusively, to evaluate its reactivity towards the substrate. Moreover, the rate of 5-HT oxidation decreases with an increase in Cu–Aβ concentration from 0.74 mM to 1.38 mM (Fig. S9 and Table S1†). Note that the Cu–Aβ concentration dependence on substrate oxidation is consistent with the higher rate of dimerization of Cu(II)–OOH to produce bis-μ-oxo dicopper(III), as observed in EPR spectroscopy (Fig. 3B). These results unambiguously support that Cu(II)–OOH is the active oxidant responsible for the oxidation of 5-HT. This is in contrast to the report by Ming *et al.*, in which they have proposed a side-on μ-peroxo dicopper(II) intermediate as the active oxidant for Cu–Aβ for substrate oxidation in the presence of H<sub>2</sub>O<sub>2</sub>.<sup>34,36</sup> Our conclusion agrees very well with the mechanism of enzymes like DβM, where the Cu(II)–OOH species or species originating from it are responsible for the chemical oxidation of amino acids and neurotransmitters.<sup>60–62</sup>

Finally, reduced Cu–Aβ can react with O<sub>2</sub>, where the Cu gets oxidized and H<sub>2</sub>O<sub>2</sub> is generated *via* disproportionation of the O<sub>2</sub><sup>−</sup> produced.<sup>11</sup> The H<sub>2</sub>O<sub>2</sub> generated from dissolved oxygen in blood can trigger the oxidation of serotonin. This is exactly the same case as indicated by the gradual appearance of the bands corresponding to the oxidized products of 5-HT when incubated with a solution of Cu–Aβ reduced with ascorbic acid in aerated buffer solutions (Fig. 6, blue), albeit the extent of oxidized HT



Scheme 3 Reaction of Cu–Aβ with 50 eq. H<sub>2</sub>O<sub>2</sub> at pH 7.

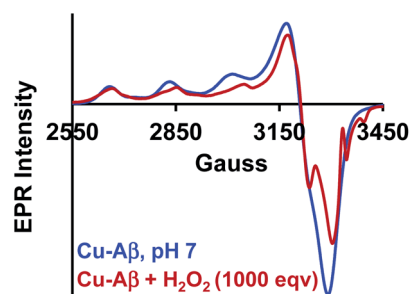


Fig. 5 EPR spectra of Cu–Aβ, blue; for the reaction of Cu–Aβ with 1000 eq. H<sub>2</sub>O<sub>2</sub>, red; in 100 mM HEPES buffer at pH 7, at 77 K.

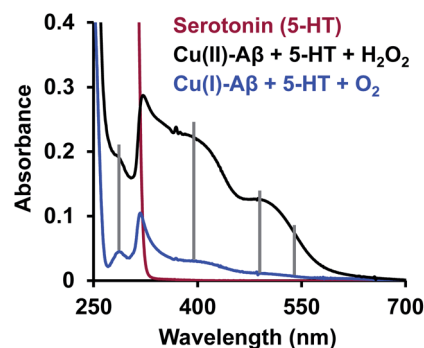
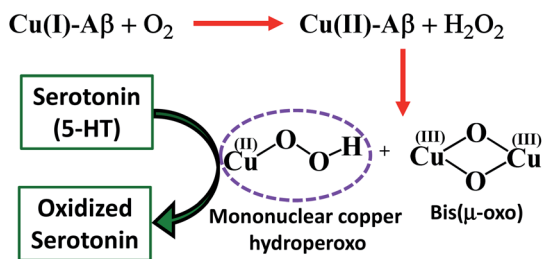


Fig. 6 Absorption spectra of serotonin (5-HT), red; oxidation of 5-HT by H<sub>2</sub>O<sub>2</sub> catalyzed by Cu(II)–Aβ, black and by O<sub>2</sub> catalyzed by Cu(I)–Aβ, blue; in 100 mM HEPES buffer at pH 7.





Scheme 5 Serotonin oxidation catalyzed by a reactive oxidant.

produced is much less under these stoichiometric conditions. Ming *et al.* have previously observed a similar result as Cu-A $\beta$  significantly accelerated the aerobic oxidation of the neurotransmitters.<sup>34</sup> Scheme 5 demonstrates the possible routes for the oxidation of serotonin.

## Conclusion

Cu-A $\beta$  oxidizes the neurotransmitter serotonin (5-HT) in the presence of H<sub>2</sub>O<sub>2</sub>. The combined absorption, EPR and resonance Raman data indicate that Cu(II)-A $\beta$  reacts with H<sub>2</sub>O<sub>2</sub> to produce bis( $\mu$ -oxo)dicopper and mononuclear copper hydroperoxo intermediates. This is the first experimental characterization of the active oxidants originating from Cu bound A $\beta$  that can oxidize neurotransmitters like serotonin (5-HT) and generate neurotoxins like tryptamine-4,5-dione, which are also observed in an AD brain. Cu(II)-A $\beta$  can be reduced by physiologically relevant reductants like ascorbic acid and this reduced Cu center can generate H<sub>2</sub>O<sub>2</sub> by reacting with dissolved oxygen, which can then oxidize 5-HT catalyzed by the Cu(II)-A $\beta$  produced. Both these pathways are accessible under physiological conditions and may account for the abnormal neurotransmission, a key pathological feature of AD.

## Conflicts of interest

There are no conflicts to declare.

## Acknowledgements

We thank DST, SERB India for financial support (grants EMR/2014/000392 and EMR/2015/0008063). A. K. N. and A. G. are funded by the University Grants Commission Fellowship. The authors thank CSS and IACS for providing HPLC facility.

## Notes and references

- 1 T. Lühns, C. Ritter, M. Adrian, D. Riek-Loher, B. Bohrmann, H. Döbeli, D. Schubert and R. Riek, *Proc. Natl. Acad. Sci. U. S. A.*, 2005, **102**, 17342.
- 2 J. J. Balbach, A. T. Petkova, N. A. Oyler, O. N. Antzutkin, D. J. Gordon, S. C. Meredith and R. Tycko, *Biophys. J.*, 2002, **83**, 1205–1216.
- 3 C. Schmidt, M. Wolff, M. Weitz, T. Bartlau, C. Korth and I. Zerr, *Arch. Neurol.*, 2011, **68**, 1124–1130.

- 4 J. Hardy and D. J. Selkoe, *Science*, 2002, **297**, 353.
- 5 F. Kametani and M. Hasegawa, *Front. Neurosci.*, 2018, **12**, 25.
- 6 L. M. F. Gomes, J. C. Bataglioli and T. Storr, *Coord. Chem. Rev.*, 2020, **412**, 213255.
- 7 A. Rauk, *Chem. Soc. Rev.*, 2009, **38**, 2698–2715.
- 8 S. Bagheri, R. Squitti, T. Haertlé, M. Siotto and A. A. Saboury, *Front. Aging Neurosci.*, 2018, **9**, 446.
- 9 C. Garza, Y. Posadas, L. Quintanar, M. Gonsebatt and R. Franco, *Antioxid. Redox Signaling*, 2018, **28**, 1669–1703.
- 10 C. Cheignon, M. Tomas, D. Bonnefont-Rousselot, P. Faller, C. Hureau and F. Collin, *Redox Biol.*, 2018, **14**, 450–464.
- 11 D. Pramanik and S. G. Dey, *J. Am. Chem. Soc.*, 2011, **133**, 81–87.
- 12 D. Pramanik, C. Ghosh and S. G. Dey, *J. Am. Chem. Soc.*, 2011, **133**, 15545–15552.
- 13 C. Ghosh and S. G. Dey, *Inorg. Chem.*, 2013, **52**, 1318–1327.
- 14 I. Pal, M. Roy and S. G. Dey, *J. Biol. Inorg. Chem.*, 2019, **24**, 1245–1259.
- 15 S. C. Drew, C. J. Noble, C. L. Masters, G. R. Hanson and K. J. Barnham, *J. Am. Chem. Soc.*, 2009, **131**, 1195–1207.
- 16 P. Dorlet, S. Gambarelli, P. Faller and C. Hureau, *Angew. Chem., Int. Ed.*, 2009, **48**, 9273–9276.
- 17 B.-k. Shin and S. Saxena, *Biochemistry*, 2008, **47**, 9117–9123.
- 18 S. Furlan, C. Hureau, P. Faller and G. La Penna, *J. Phys. Chem. B*, 2012, **116**, 11899–11910.
- 19 E. I. Solomon, D. E. Heppner, E. M. Johnston, J. W. Ginsbach, J. Cirera, M. Qayyum, M. T. Kieber-Emmons, C. H. Kjaergaard, R. G. Hadt and L. Tian, *Chem. Rev.*, 2014, **114**, 3659–3853.
- 20 R. H. Holm, P. Kennepohl and E. I. Solomon, *Chem. Rev.*, 1996, **96**, 2239–2314.
- 21 J. P. Klinman, *Chem. Rev.*, 1996, **96**, 2541–2562.
- 22 A. Beliaev, H. Ferreira, D. A. Learmonth and P. Soares-da-Silva, *Curr. Enzyme Inhib.*, 2009, **5**, 27–43.
- 23 J. P. Evans, K. Ahn and J. P. Klinman, *J. Biol. Chem.*, 2003, **278**, 49691–49698.
- 24 J. P. Klinman, *J. Biol. Chem.*, 2006, **281**, 3013–3016.
- 25 R. Kandimalla and P. H. Reddy, *J. Alzheimer's Dis.*, 2017, **57**, 1049–1069.
- 26 D. M. Bowen, *AGE*, 1988, **11**, 104–109.
- 27 S. A. Lyness, C. Zarow and H. C. Chui, *Neurobiol. Aging*, 2003, **24**, 1–23.
- 28 S. G. Snowden, A. A. Ebshiana, A. Hye, O. Pletnikova, R. O'Brien, A. Yang, J. Troncoso, C. Legido-Quigley and M. Thambisetty, *J. Alzheimer's Dis.*, 2019, **72**, 35–43.
- 29 H. Förstl and P. Fischer, *Eur. Arch. Psychiatr. Clin. Neurosci.*, 1994, **244**, 252–260.
- 30 S. Kaur, G. DasGupta and S. Singh, *Neurophysiology*, 2019, **51**, 293–309.
- 31 M. Z. Wrona and G. Dryhurst, *Chem. Res. Toxicol.*, 1998, **11**, 639–650.
- 32 L. Volicer and P. B. Crino, *Neurobiol. Aging*, 1990, **11**, 567–571.
- 33 P. B. Crino, B. A. Vogt, J.-C. Chen and L. Volicer, *Brain Res.*, 1989, **504**, 247–257.
- 34 G. F. Z. da Silva and L.-J. Ming, *Angew. Chem., Int. Ed.*, 2007, **46**, 3337–3341.



- 35 G. F. Z. da Silva and L.-J. Ming, *Angew. Chem., Int. Ed.*, 2005, **44**, 5501–5504.
- 36 G. F. da Silva, V. Lykourinou, A. Angerhofer and L. J. Ming, *Biochim. Biophys. Acta*, 2009, **1792**, 49–55.
- 37 G. F. da Silva, W. M. Tay and L. J. Ming, *J. Biol. Chem.*, 2005, **280**, 16601–16609.
- 38 M. Z. Wrona, Z. Yang, M. McAdams, S. O'Connor-Coates and G. Dryhurst, *J. Neurochem.*, 1995, **64**, 1390–1400.
- 39 V. F. Ximenes, G. J. Maghzal, R. Turner, Y. Kato, C. C. Winterbourn and A. J. Kettle, *Biochem. J.*, 2009, **425**, 285–293.
- 40 C. E. Elwell, N. L. Gagnon, B. D. Neisen, D. Dhar, A. D. Spaeth, G. M. Yee and W. B. Tolman, *Chem. Rev.*, 2017, **117**, 2059–2107.
- 41 L. M. Mirica, X. Ottenwaelder and T. D. P. Stack, *Chem. Rev.*, 2004, **104**, 1013–1046.
- 42 E. I. Solomon, P. Chen, M. Metz, S.-K. Lee and A. E. Palmer, *Angew. Chem., Int. Ed.*, 2001, **40**, 4570–4590.
- 43 F. Nistri, M. Chino, O. Maglio, A. Bhagi-Damodaran, Y. Lu and A. Lombardi, *Chem. Soc. Rev.*, 2016, **45**, 5020–5054.
- 44 J. A. Halfen, S. Mahapatra, E. C. Wilkinson, S. Kaderli, V. G. Young, L. Que, A. D. Zuberbühler and W. B. Tolman, *Science*, 1996, **271**, 1397.
- 45 M. J. Henson, M. A. Vance, C. X. Zhang, H.-C. Liang, K. D. Karlin and E. I. Solomon, *J. Am. Chem. Soc.*, 2003, **125**, 5186–5192.
- 46 S. Mahapatra, J. A. Halfen, E. C. Wilkinson, G. Pan, C. J. Cramer, L. Que Jr and W. B. Tolman, *J. Am. Chem. Soc.*, 1995, **117**, 8865–8866.
- 47 E. I. Solomon, J. W. Ginsbach, D. E. Heppner, M. T. Kieber-Emmons, C. H. Kjaergaard, P. J. Smeets, L. Tian and J. S. Woertink, *Faraday Discuss.*, 2011, **148**, 11–108.
- 48 D. J. E. Spencer, A. M. Reynolds, P. L. Holland, B. A. Jazdzewski, C. Duboc-Toia, L. Le Pape, S. Yokota, Y. Tachi, S. Itoh and W. B. Tolman, *Inorg. Chem.*, 2002, **41**, 6307–6321.
- 49 P. L. Holland, C. J. Cramer, E. C. Wilkinson, S. Mahapatra, K. R. Rodgers, S. Itoh, M. Taki, S. Fukuzumi, L. Que and W. B. Tolman, *J. Am. Chem. Soc.*, 2000, **122**, 792–802.
- 50 N. Lehnert, K. Fujisawa and E. I. Solomon, *Inorg. Chem.*, 2003, **42**, 469–481.
- 51 Y. J. Choi, K.-B. Cho, M. Kubo, T. Ogura, K. D. Karlin, J. Cho and W. Nam, *Dalton Trans.*, 2011, **40**, 2234–2241.
- 52 P. Chen, K. Fujisawa and E. I. Solomon, *J. Am. Chem. Soc.*, 2000, **122**, 10177–10193.
- 53 B. Kim, D. Jeong, T. Ohta and J. Cho, *Commun. Chem.*, 2019, **2**, 81.
- 54 P. J. Mak, W. Thammawichai, D. Wiedenhoft and J. R. Kincaid, *J. Am. Chem. Soc.*, 2015, **137**, 349–361.
- 55 N. Lehnert, F. Neese, R. Y. N. Ho, L. Que and E. I. Solomon, *J. Am. Chem. Soc.*, 2002, **124**, 10810–10822.
- 56 R. Y. N. Ho, G. Roelfes, B. L. Feringa and L. Que, *J. Am. Chem. Soc.*, 1999, **121**, 264–265.
- 57 A. Ghatak, S. Bhunia and A. Dey, *ACS Catal.*, 2020, **10**, 13136–13148.
- 58 C. Citek, S. Herres-Pawlis and T. D. P. Stack, *Acc. Chem. Res.*, 2015, **48**, 2424–2433.
- 59 M. T. Kieber-Emmons, J. W. Ginsbach, P. K. Wick, H. R. Lucas, M. E. Helton, B. Lucchese, M. Suzuki, A. D. Zuberbühler, K. D. Karlin and E. I. Solomon, *Angew. Chem., Int. Ed.*, 2014, **53**, 4935–4939.
- 60 P. Chen and E. I. Solomon, *J. Am. Chem. Soc.*, 2004, **126**, 4991–5000.
- 61 A. Crespo, M. A. Martí, A. E. Roitberg, L. M. Amzel and D. A. Estrin, *J. Am. Chem. Soc.*, 2006, **128**, 12817–12828.
- 62 P. Chen and E. I. Solomon, *Proc. Natl. Acad. Sci. U. S. A.*, 2004, **101**, 13105–13110.

